Standard surface-reflectance model and illuminant estimation

Shoji Tominaga

Faculty of Engineering, Osaka Electro-Communication University, 18-8 Hatsu-cho, Neyagawa, Osaka 572, Japan

Brian A. Wandell

Department of Psychology, Stanford University, Stanford, California 94305

Received May 2, 1988; accepted November 17, 1988

In the standard reflectance model for inhomogeneous materials it is assumed that light is reflected by two independent mechanisms. One component is reflected at the interface of the material and air. Light reflected by this mechanism does not interact with surface colorant, and its spectral composition is assumed to equal that of the incident light. The second component is reflected after entering and interacting with the subsurface structure of the material. This interaction substantially changes the spectral composition of the reflected light. We adopt a vector analysis technique for testing the standard reflectance model. Further, we develop a computational method to determine the components of the observed spectra, and we obtain an estimate of the illuminant without using a reference white standard. Finally, we evaluate the accuracy of the standard model and the feasibility of the illuminant spectral estimation by using several test objectives.

1. INTRODUCTION

The visual information that we use to judge the color appearance of an object is derived from the light reflected from the object and the light reflected from nearby objects. The spectral composition of the reflected light depends on the surface-reflectance properties of the objects and the spectral composition of the ambient lighting. For many broadband light sources an object's color appearance often is predicted more closely by the object's surface reflectance than by the spectral composition of the light reflected from the object, which depends on the ambient lighting. This rough approximation, that the effects of the spectral variation of the ambient lighting are discounted and the object appearance is approximately constant, is called color constancy.

The human ability to discount the effect of some changes in the ambient lighting has motivated the construction of a number of algorithms to demonstrate how this feat may be accomplished. In most of these algorithms significant assumptions are made about the surface-reflectance properties of objects. Some of these algorithms are designed to estimate object surface-reflectance functions from the responses recorded by a small number of spectrally distinct sensors even when the ambient lighting is unknown. Within this group of algorithms, some are based on models of surface specularity,[1-3] and others are based on other assumptions concerning the properties of surface-reflectance functions.[4-6] Accurate modeling of surface-reflectance functions has become important in the field of computer graphics,[7] where knowledge of surface-reflectance properties permits more accurate rendering of object appearance.

From these algorithms we can now appreciate the close relationship between the mathematical structure of the surface-reflectance functions and the algorithms that can accurately estimate or render surface properties. As we learn more about the mathematical properties of the surface-reflectance functions, reflectance estimation can be accomplished by using fewer sensors or using more-efficient algorithms.

In the fields of computer graphics and computer vision, a few central ideas are used widely to summarize the mathematical structure of surface-reflectance functions on inhomogeneous substances, which are substances composed of different component materials, such as a vehicle at the surface layer and embedded pigments at the colorant layer. For example, plastics and paints are inhomogeneous. Typical examples of homogeneous objects are metals and crystals. For homogeneous materials, the incident light suffers no scattering; the light is reflected in accordance with Fresnel's law.[8] Homogeneous objects are not represented by a simple reflectance model.

In all reflectance models it is postulated that light reflected from an object is composed of light reflected from two different physical paths. Some light is reflected at the interface between the object's surface and the air. This type of reflection is mirrorlike; light reflected in this way from a point source can be seen only over a narrow range of viewing geometries. This light is said to be the specular (or interface) reflection.

The second reflectance path occurs for light that crosses the object's interface. Once the light enters the pigment colorant layer, significant scattering of the light among the pigment particles in this layer occurs. The light is observed only after it crosses the surface boundary again into the air. Light reflected from this type of path is said to be the diffuse (or subsurface) reflection.

The characterization of the reflected light by the additive component of a small number of terms is implicit in the studies of many authors and was summarized well by Cook and Torrance.[7] Beyond this general formulation, Shafer[9]

0740-3232/89/040576-09$02.00

proposed that, for measurement purposes, specifically for computer vision, several approximations are useful. These approximations are based on the assumption that for inhomogeneous materials the wavelength functions are invariant with respect to the angle of the incident light. Shafer refers to these ideas as the dichromatic reflection model. We believe that the ideas draw on such widely held approximations that the collection of ideas might well be called the standard reflectance model.

First, in the standard reflectance model it is assumed that the ratio between the spectral composition of the light that enters the material and the light that leaves the material is the same for all angles. This ratio of the incident and reflected light is the surface-reflectance function of the diffuse component. Second, in the standard model the specularly reflected light is approximated as being invariant, except for a change in intensity, with respect to viewing geometry. Fresnel's equations for specular reflectance do vary with respect to angle, but this variation is asserted to be sufficiently small (see, e.g., Ref. 9) as to be negligible for many observational conditions.

Although the standard reflectance model is used widely to describe empirical properties of data, there are relatively few experimental results to evaluate the adequacy of the model. Recently Klinker *et al.*[1] used the model to analyze color images including highlights. Their measurements are based on three-color-filter (RGB) camera data. Lee *et al.*[10] presented some spectral wavelength experimental data to show that the standard reflectance model is reasonable for some objects. These models were based on the assumption of the two components of light reflection.

Given the importance of the model for applications, we believed that some further empirical examination of the model and some further examination of algorithms that depend on the model would be of value. In this paper we describe new measurements of the spectral power distributions of lights reflected from objects under a variety of geometric conditions. We use a principal-component decomposition of these observed spectra to test the adequacy of the two-component reflection model.

Several authors have pointed out that, if the standard model is correct and if the spectral composition of the specular component of the light is the same as the spectral composition of the incident light,[11] then some simple algorithms can be designed to estimate the spectral power distribution of the light from sensor data. For example, Lee[2] proposed a method for computing the illuminant chromaticity from the color coordinates of specular highlights, as did D'Zmura and Lennie.[3] In this paper we extend the work of these authors. We define an algorithm that permits one to combine information from two or more surfaces to estimate the spectral composition of the ambient lighting. We show that the problem of estimating the illuminant spectrum is reduced to that of finding the common spectral information from all the measurements from the surfaces.

The illuminant estimation method that we describe can be useful for remote sensing applications. When we measure light reflected from objects at a distance, say, 100 km away, we cannot place a white standard at the remote site. Our method can be used to infer the illuminant spectral power distributions at remote image locations. However, the reader should note that the standard reflectance model applies to inhomogeneous surfaces and is not appropriate for homogeneous materials, such as metallic surfaces. Highlights from metallic surfaces are not equal to the illuminant spectral power distribution.

In Section 2 we give a mathematical formulation of the standard reflectance model. In Section 3 we state the basic principle of our spectral analysis approach to the color reflection problem. The computational method is developed in Section 4. In Section 5 we present our experimental results. The performance and the application are discussed in Section 6.

2. STANDARD REFLECTANCE MODEL

It is generally supposed that light reflected from an object surface can be decomposed into two additive components, the interface reflection and the subsurface reflection (see Fig. 1). In the general case the radiance of the reflected light Y is described as a function of wavelength and geometric parameters,

$$Y(\theta, \lambda) = Y_I(\theta, \lambda) + Y_S(\theta, \lambda), \tag{1}$$

where the wavelength λ ranges over a visible spectrum and the parameters θ include the direction angles needed for describing a reflection geometry, such as the incident angle, the viewing angle, and the phase angle. The subscripts I and S denote the interface and subsurface components, respectively. The key additional assumption of the standard reflectance model is the separability between the wavelength composition and the geometrical conditions.

Additivity and Separability

The spectral composition of each reflected light component is independent of the geometric conditions; that is, the respective components of the spectral radiances Y_I and Y_S are separated into the wavelength factor and the geometric variables as follows:

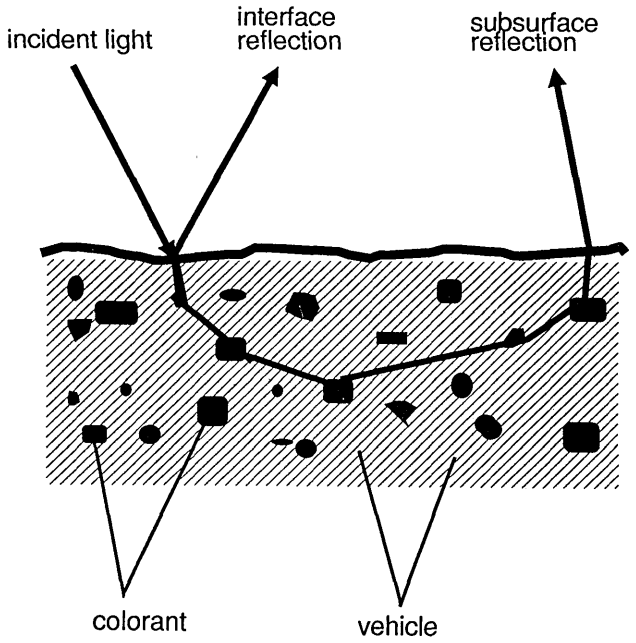

Fig. 1. Light reflected from a surface is modeled as the sum of two components. Each component represents a different light path.

$$Y(\theta, \lambda) = c_I(\theta)L_I(\lambda) + c_S(\theta)L_S(\lambda). \quad (2)$$

The terms $L_I(\lambda)$ and $L_S(\lambda)$ are the spectral power distributions of the interface and subsurface reflection components, respectively. The terms $c_I(\theta)$ and $c_S(\theta)$ are the geometric scale factors.

Equation (2) states that the color signals from an inhomogeneous object are described by the linear combination of two spectral power distributions. The weighting coefficients of each term are geometric scale factors. The important aspect of this assumption is that the spectral composition of each of the reflection components is unchanged as the viewing angle varies.

If we wish to estimate the surface-reflectance functions from the color signal Y, then we must express the reflection model in terms of the surface reflectance of an object and the spectral power distribution of an incident light. Let $S_I(\lambda)$ and $S_S(\lambda)$ be the spectral surface reflectances for the two components. Let $E(\lambda)$ be the spectral power distribution of the incident light. We can represent the reflected light as

$$Y(\theta, \lambda) = c_I(\theta)S_I(\lambda)E(\lambda) + c_S(\theta)S_S(\lambda)E(\lambda). \quad (3)$$

The interface component of reflectance $S_I(\lambda)$ is determined by Fresnel's law. If the refractive index at the surface is constant over the visible wavelength, then the interface component is independent of wavelength. It was reported that many types of material serving as vehicles are some sort of oil and have constant indices of refraction.[2] For these surfaces, the specular reflection appears to have the same color as the illuminant source. A satisfactory approximation for many materials is as follows.

Constant Specular Reflectance

The interface component of surface spectral reflectance is constant over the visible wavelength as $S_I(\lambda) = \text{constant}$.

Note that, from radiometric concepts, the spectral reflectance has the dimension of inverse nanometer inverse steradian ($nm^{-1}\,sr^{-1}$). However, the data analysis of color signals is done in relative values through this paper, and thus the physical dimensions do not play a significant role.

3. TEST OF THE STANDARD REFLECTANCE MODEL

In the standard reflectance model it is assumed that the color signals $Y(\theta, \lambda)$ can be expressed as a linear combination of the two component vectors of light reflection $L_I(\lambda)$ and $L_S(\lambda)$. The two vectors $L_I(\lambda)$ and $L_S(\lambda)$ span a two-dimensional plane, that is, a subspace, of the possible observations. All the color signals observed from an inhomogeneous surface should fall in a subspace that lies on this plane. We call this plane the color-signal plane P. Figure 2 shows the plane as a parallelogram. All the color signals must be located inside the parallelogram. It is important to note that this color-signal plane is defined by both the object surface reflectance and the spectral power distribution of the illuminant. The color-signal plane will change with different illuminants. The first test of the standard reflectance model, then, is to determine whether the color signals observed from an inhomogeneous material fall within a two-dimensional subspace of the set of possible color signals.

If the key requirement of the standard reflectance model is met, namely, additivity and separability, then we may proceed to test the additional assumption of constant specular reflectance. An important practical consequence of this assumption is that the color-signal information can be used to estimate the spectral power distribution of the illuminant. Conversely, the reliability of the estimate may also be used to test the assumption of constant specular reflectance, which is the method that we use here.

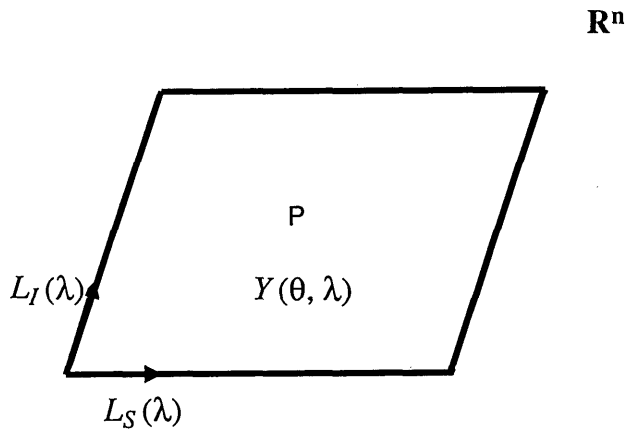

Fig. 2. Color signal plane by a linear combination of the interface reflection component $L_I(\lambda)$ and the subsurface reflection component $L_S(\lambda)$.

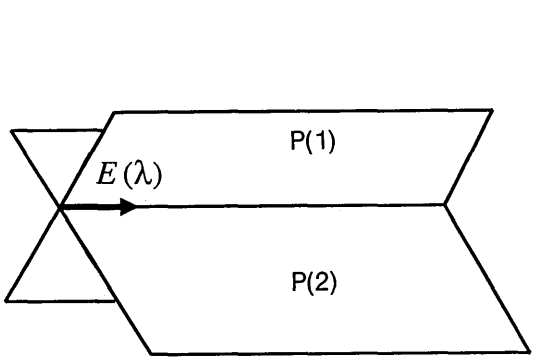

Fig. 3. The intersection of two color-signal planes P(1) and P(2).

Suppose that we measure color signals reflected from two surfaces of inhomogeneous material under the same light source. When we measure the reflected lights with different geometric conditions, then by the first assumption the data will form two different color-signal planes P(1) and P(2) in the space. If the assumption of constant specular reflectance is true, then the spectral power distributions of color signals for the surfaces can be described as follows:

$$Y_1(\theta, \lambda) = c_{I_1}(\theta)E(\lambda) + c_{S_1}(\theta)S_{S_1}(\lambda)E(\lambda), \quad (4)$$

$$Y_2(\theta, \lambda) = c_{I_2}(\theta)E(\lambda) + c_{S_2}(\theta)S_{S_2}(\lambda)E(\lambda). \quad (5)$$

The planes P(i)(i = 1, 2) are constructed by a set of two vectors $[E(\lambda), S_{S_i}(\lambda)E(\lambda)]$. Note that the illuminant vector $E(\lambda)$ is contained in both planes. This vector represents the common spectral information that is due to the light source. The two planes must intersect at this vector, as shown in Fig. 3.

We test the assumption of constant specular reflectance as follows. If the assumption is true, then two color-signal

planes from objects under the same illuminant must intersect. Moreover, the vector of their intersection must be in the direction of the illuminant vector. As a useful practical consequence, the standard reflectance model along with the assumption of constant specular reflectance predicts that we can estimate the illuminant spectrum from the color signals reflected from two object surfaces. The estimation problem of an illuminant spectrum can be reduced to a computational problem of finding an intersection of two color-signal planes.

The above-described property can be extended to the case of many surfaces. If there are three or more object surfaces of inhomogeneous material, then more than three color-signal planes are constructed in a vector space of the spectral power distributions. All the planes must intersect at only a common line, which corresponds to the illuminant spectrum.

The points of the present spectral analysis are summarized as follows:

(1) If the assumption of additivity and separability of the reflection model is true, the spectral data must form a two-dimensional subspace.

(2) If the assumption of constant reflectance is true, then the color signal planes from different object surfaces intersect at a common line in the direction of the illuminant.

We evaluate the standard reflectance model by measuring the spectral power distributions of light reflected from inhomogeneous material at various geometric angles. For any single surface material, we test to determine whether the color signals are described well by a plane. We then test to determine whether the subspaces for two different materials intersect and whether the intersection falls in the direction of the illuminant. Notice that strong specular highlights are not required to determine the color-signal plane. In this analysis we require only a wide range of measurements that includes specular and diffuse components. From this pattern of results, we should be able to obtain reliable estimates of the illuminant.

4. COMPUTATIONAL METHODS

A. Determining a Color-Signal Plane

Let us assume that we observe m color signals reflected from an object surface under various geometric conditions but with a constant illuminant. We sample each spectral power distribution at n points in the visible-wavelength region. The m color signals are represented by n-dimensional column vectors denoted by $\mathbf{y}_i$ ($i = 1, 2, \ldots, m$). If a set of data vectors falls in a subspace, their normalized representations fall in the same plane. Thus the absolute radiance values are not necessary to our analysis. We perform all our calculations by using the normalized spectral power distributions; that is, we normalize the measurements to unit power in the sense that $\|y_i\|^2 = 1$. The notation $\|\mathbf{y}\|^2$ is defined as $\mathbf{y}^T\mathbf{y}$, where T denotes a matrix (or vector) transposition. All the normalized spectral power distributions are summarized in an $n \times m$ matrix $\mathbf{Y}$ defined by

$$\mathbf{Y} = [\mathbf{y}_1, \mathbf{y}_2, \ldots, \mathbf{y}_m]. \tag{6}$$

We use the singular-value decomposition (SVD) to determine a color signal plane from the observed light spectra. The SVD is a useful tool for orthogonal decomposition of general rectangular matrices. The application to data analysis is similar to the idea of the well-known principal-component analysis. The SVD of the matrix $\mathbf{Y}$ is given in the following form[12]:

$$\mathbf{Y} = \mathbf{U}\Sigma\mathbf{V}^T, \tag{7}$$

or, equivalently,

$$\mathbf{Y} = \sigma_1\mathbf{u}_1\mathbf{v}_1{}^T + \sigma_2\mathbf{u}_2\mathbf{v}_2{}^T + \ldots + \sigma_m\mathbf{u}_m\mathbf{v}_m{}^T, \tag{8}$$

where $\mathbf{U}$ ($= [\mathbf{u}_1, \mathbf{u}_2, \ldots, \mathbf{u}_n]$) and $\mathbf{V}$ ($= [\mathbf{v}_1, \mathbf{v}_2, \ldots, \mathbf{v}_n]$) are the $n \times m$ left-hand singular matrix and the $m \times m$ right-hand singular matrix, respectively, and Σ is the $m \times m$ diagonal matrix with elements of the singular values $\sigma_1, \sigma_2, \ldots, \sigma_m$. The n-dimensional left-hand singular vectors $\mathbf{u}_1, \mathbf{u}_2, \ldots, \mathbf{u}_m$ and the m-dimensional right-hand singular vectors $\mathbf{v}_1, \mathbf{v}_2, \ldots, \mathbf{v}_m$ are orthonormal eigenvectors of $\mathbf{YY}^T$ and $\mathbf{Y}^T\mathbf{Y}$, respectively. The singular values σ_i are the square roots of the eigenvalues of $\mathbf{YY}^T$ or $\mathbf{Y}^T\mathbf{Y}$. We assume the descending order $\sigma_i \geq \sigma_{i+1}$.

The dimensionality of the space spanned by the measured color signals can be estimated from the rank of the matrix $\mathbf{Y}$. Let us denote the n-dimensional vector space by the symbol $\mathbf{R}^n$. The measured color signals then fall into a two-dimensional subspace of $\mathbf{R}^n$ when the rank of $\mathbf{Y}$ is 2. This occurs when $\sigma_1 \geq \sigma_2 > 0$ and $\sigma_3 = \sigma_4 = \ldots = \sigma_m = 0$. In practice these strict equations are not satisfied perfectly because nonzero singular values appear as a result of measurement noise and computer roundoff error. A fairly reliable way to estimate the rank is to compare the singular values by using the following performance index:

$$I(K) = \frac{\sum_{i=1}^{K} \sigma_i^2}{\sum_{i=1}^{m} \sigma_i^2} = \frac{\sum_{i=1}^{K} \sigma_i^2}{m}. \tag{9}$$

By hypothesis we expect that $I(2) = 1.0$. If $I(1) = 1.0$, then the measured data are one dimensional. In this case the observation conditions reveal only one component of the interface and subsurface reflections from an object. If $I(2) \ll 1$, then the data have a higher dimensionality than 2. In this case we must consider whether the object might be a homogeneous material or whether the standard reflectance model is in error for this material.

The left-hand singular vectors $\mathbf{u}_1$ and $\mathbf{u}_2$ are a set of basis vectors that span a two-dimensional subspace of $\mathbf{R}^n$. When $I(2) = 1$, all the measured spectral power distributions are described in a linear combination of $\mathbf{u}_1$ and $\mathbf{u}_2$, since

$$\mathbf{y}_i = c_{i1}\mathbf{u}_1 + c_{i2}\mathbf{u}_2 \qquad (i = 1, 2, \ldots, m), \tag{10}$$

where $c_{ij} = \sigma_j v_{ij}$ ($j = 1, 2$). Therefore the color-signal plane of the object surface can be determined from

$$P = \{\mathbf{y} \quad | \mathbf{y} = c_1\mathbf{u}_1 + c_2\mathbf{u}_2, \quad c_i \in R\}. \tag{11}$$

The set R is a set of real numbers such that $\mathbf{y}$ is nonnegative and physically realizable.

B. Estimating an Illuminant Spectral Distribution

Let us assume that two object surfaces are observed under the same light source. Two color-signal planes are determined from the SVD's of the two data sets. The vectors $\mathbf{u}_1$ and $\mathbf{u}_2$ are an orthonormal basis that defines the color-signal plane. [Note that these vectors do not correspond to the physically defined components of the two reflections, $L_I(\lambda)$ and $L_S(\lambda)$.]

Let $[\mathbf{u}_1(1), \mathbf{u}_2(1)]$ and $[\mathbf{u}_1(2), \mathbf{u}_2(2)]$ be the basis vectors of the color-signal planes P(1) and P(2). Since the intersection line must lie in both P(1) and P(2), we have the relation

$$c_1\mathbf{u}_1(1) + c_2\mathbf{u}_2(1) = c_1'\mathbf{u}_1(2) + c_2'\mathbf{u}_2(2). \tag{12}$$

This relationship is equivalent to the homogeneous equation

$$[\mathbf{u}_1(1), \mathbf{u}_2(1), \mathbf{u}_1(2), \mathbf{u}_2(2)] \begin{bmatrix} c_1 \\ c_2 \\ -c_1' \\ -c_2' \end{bmatrix} = 0. \tag{13}$$

A nontrivial solution of Eq. (13) defines the intersection of the planes. A reliable solution method is to apply the SVD algorithm to the above $n \times 4$ matrix again. We then have

$$[\mathbf{u}_1(1), \mathbf{u}_2(1), \mathbf{u}_1(2), \mathbf{u}_2(2)] = [\mathbf{a}_1, \mathbf{a}_2, \mathbf{a}_3, \mathbf{a}_4] \begin{bmatrix} \lambda_1 & 0 & 0 & 0 \\ 0 & \lambda_2 & 0 & 0 \\ 0 & 0 & \lambda_3 & 0 \\ 0 & 0 & 0 & \lambda_4 \\ - & - & - & - \end{bmatrix} \times [\mathbf{b}_1, \mathbf{b}_2, \mathbf{b}_3, \mathbf{b}_4]^T, \tag{14}$$

where the definitions of $\mathbf{a}_i$, $\mathbf{b}_i$, and λ_i ($i = 1, 2, 3, 4$) correspond to those of $\mathbf{u}_i$, $\mathbf{y}_i$, and σ_i in Eq. (8). If $\lambda_4 = 0$ and $\lambda_3 > 0$ (i.e., rank = 3), the planes P(1) and P(2) intersect in a line in the n-dimensional space $\mathbf{R}^n$. The vector $\mathbf{b}_4$ is a solution for the vector at the intersection. The intersection line is described by the elements of $\mathbf{b}_4$ as

$$\mathbf{e}_1 = \sqrt{2}[b_{41}\mathbf{u}_1(1) + b_{42}\mathbf{u}_2(1)] \tag{15}$$

or

$$\mathbf{e}_2 = -\sqrt{2}[b_{43}\mathbf{u}_1(2) + b_{44}\mathbf{u}_2(2)], \tag{16}$$

where the line vectors are normalized as $\|\mathbf{e}_1\|^2 = \|\mathbf{e}_2\| = 1$. The signs of the coefficients b_{4i} are chosen so that the components of the illuminant vectors $\mathbf{e}_1$ and $\mathbf{e}_2$ are positive, consistent with the requirement that the illuminants be physically realizable. For example, when the right-hand side of Eq. (15) is negative, the signs of both b_{41} and b_{42} are reversed.

In real measurement, the value of λ_4 will not be exactly zero. However, we expect it to be small if the second condition, that of constant specularity reflectance, is satisfied. The same performance index, $I(K)$, may be used to evaluate the hypothesis in this case as well. We can regard $\mathbf{e}_1$ and $\mathbf{e}_2$ as the estimates of the spectral power distribution $E(\lambda)$ in planes P(1) and P(2), respectively. A reliable estimate $\mathbf{e}$ of the illuminant spectrum is obtained from the mean

$$\hat{\mathbf{e}} = \frac{(\mathbf{e}_1 + \mathbf{e}_2)}{2}. \tag{17}$$

The above procedure can be extended straightforwardly to the case of more than three object surfaces under the same light source. The computation to obtain an estimate is based on the repetition of the process presented here for every pair of objects in a scene.

5. EXPERIMENTS

To test the standard model experimentally and to evaluate the precision of the computational methods, we measured the light reflected from plastics and fruits under two different lighting conditions. The light sources were a flood lamp, for a daylight photograph, and a tungsten halogen lamp from a slide projector.

A. Measurement

The objects were placed on a table covered with a black cloth in a black room. The light sources were placed at the same height as the objects for a horizontal projection of the illuminant. Figure 4 shows a monochrome scene of a red plastic cup (left) and a green plastic ashtray (right), ~80 cm apart, illuminated with a flood lamp. Specular highlights are seen clearly at several parts of the surfaces. We used a spectroradiometer to measure the spectral power distributions of the reflected light. The spectroradiometer was placed ~130 cm from the objects and at the same height. The angle between the illumination and the viewing directions was 30 deg.

The surface of each plastic object is uniform and smooth. We measured the spectral radiance reflected from many spots on the surfaces by the angle of the spectroradiometer changing slightly. The power of the reflected light depends greatly on the viewing angle because the intensity in the highlights is several orders of magnitude greater than the intensity in the matte areas. The dynamic range of the spectrometer (and *a fortiori* that of conventional digitizing cameras) does not allow us to make all our measurements with a fixed aperture size. As we measured different positions we increased the aperture size from 6 min. to 1 deg. About half of the measuring spots were selected near the highlight areas and thus contained significant specular contributions. The other spots were from the matte areas and

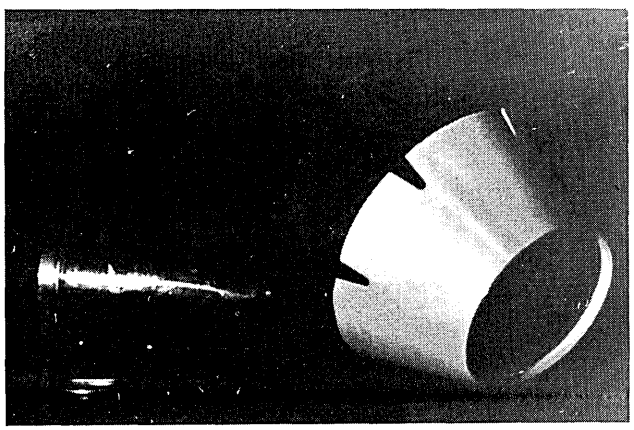

Fig. 4. A red cup (left) and a green ashtray (right) of plastic illuminated by a flood lamp.

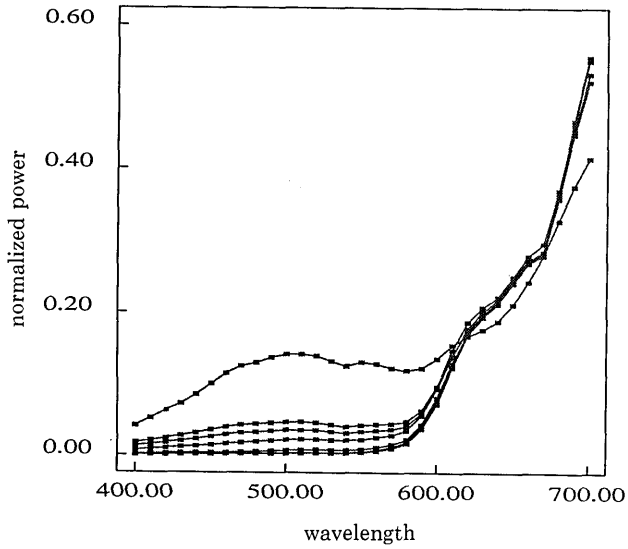

Fig. 5. Normalized curves of the measured spectra of the red plastic cup.

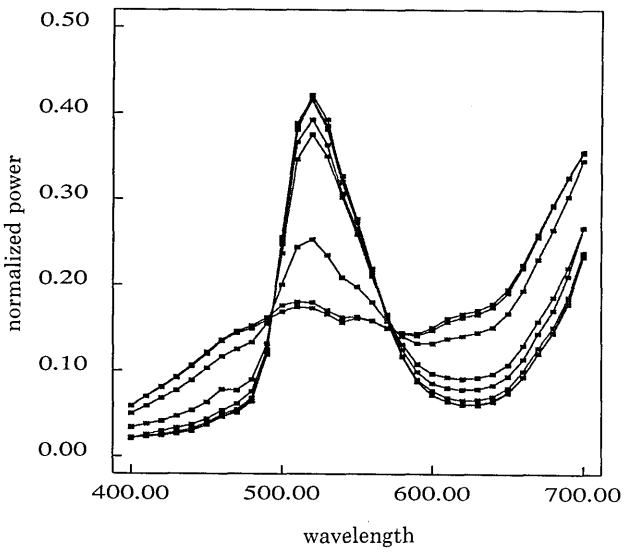

Fig. 6. Normalized curves of the measured spectra of the green plastic ashtray.

thus contained only small or no specular contributions. All the spots were confirmed visually in advance to have the same color appearance under an ordinary lighting condition without specular reflection. We believe, therefore, that variations in the measurements depend only on the geometric factors.

Figure 5 shows the normalized curves of the spectral power distributions measured at nine different spots on the red cup surface. One well-separated curve in the figure corresponds to the strongest highlight spectrum. Figure 6 shows the normalized curves measured at eight spots on the green ashtray surface. These data were obtained separately to eliminate any possible interreflections between the two objects.

Next, we observed fruits with a measuring arrangement similar to that used for the plastics but with a different light source. Figure 7 shows the scene of an apple (left) and a lemon (right), illuminated by a slide projector lamp and ~100 cm apart. It should be noted that the surface conditions of these natural products are quite different from those of the plastic industrial products. The skins of fruits are covered with a waxy tissue, and some of the light reflects at the interface. However, the surfaces are not so hard and smooth that a mirrorlike specular reflection is observed. In Fig. 7 only a weak glossy reflection appears on the lemon surface. A detailed inspection, moreover, shows that the glossy areas consist of fine textures and that the colors are not necessarily the same from a microscopic point of view.

Figures 8 and 9 show the normalized curves of the spectral power distributions measured at 10 different spots on the surfaces of the apple and the lemon, respectively. The spectral curves from the apple are separated into two types of pattern. There is relatively little variation in the spectral curves of the lemon because the glossy points are relatively small compared with the aperture size of the measurement instrument.

B. Results

The measured spectral data have been analyzed according to the computation procedure in Section 4.

1. *Plastics*

First, a 31 × 9 observation matrix **Y** for the red cup was constructed from the normalized spectral curves $\mathbf{y}_1$–$\mathbf{y}_9$, in which each curve was sampled at intervals of 10 nm. The SVD of **Y** gave the singular values of $\sigma_1 = 2.9627$, $\sigma_2 = 0.4698$, $\sigma_3 = 0.0389, \ldots$. The performance index was $I(1) = 0.9753$ for the first component only and $I(2) = 0.9998$ for the first two components. The contributions of the remaining seven components were negligibly small. From this result, we accept the hypothesis that the color-signal space measured from the red cup spans a 2-dimensional subspace of the 31-dimensional measured vector space. Figure 10 shows curves of the basis vectors $\mathbf{u}_1$ and $\mathbf{u}_2$. These curves are the principal-component curves for the measured spectral curves; that is, all the curves in Fig. 5 can be approximated with good accuracy by a linear combination of $\mathbf{u}_1$ and $\mathbf{u}_2$. These vectors determine P(1).

Next, a 31 × 8 observation matrix **Y** for the green ashtray was decomposed into its principal components. In the same

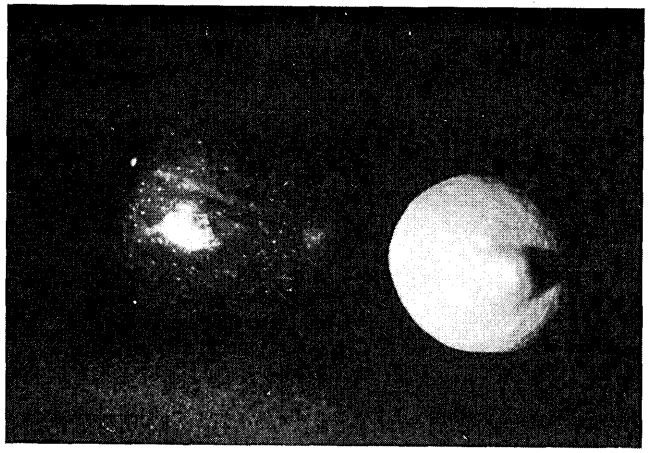

Fig. 7. An apple (left) and a lemon (right) illuminated by a tungsten halogen lamp from a slide projector.

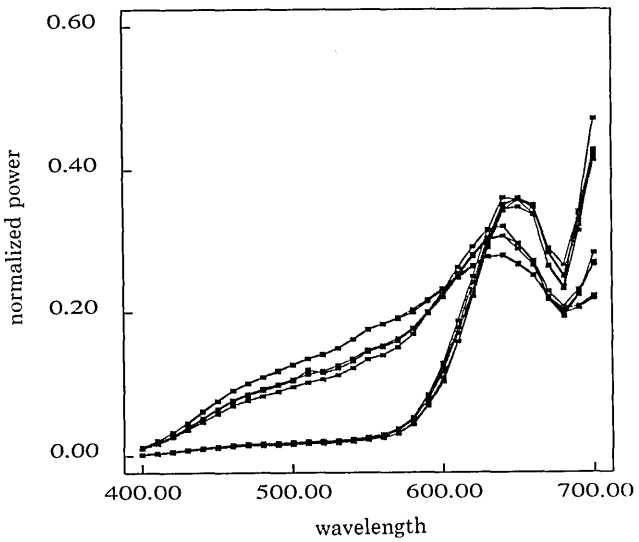

Fig. 8. Normalized curves of the measured spectra of the apple.

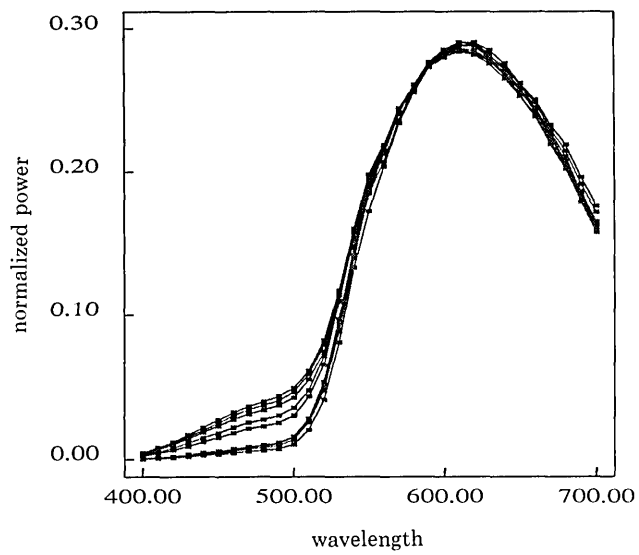

Fig. 9. Normalized curves of the measured spectra of the lemon.

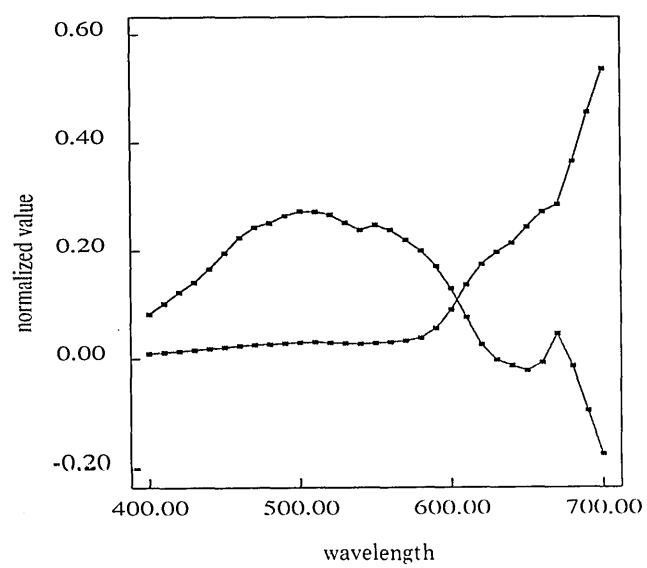

Fig. 10. Basis curves of the measured spectra of the red plastic cup.

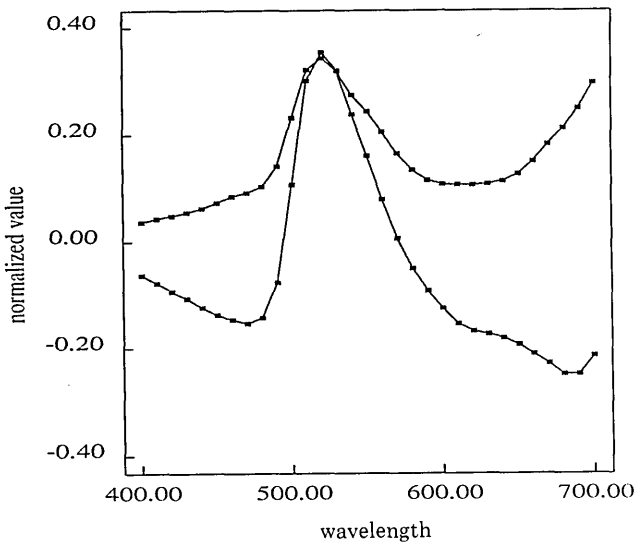

Fig. 11. Basis curves of the measured spectra of the green plastic ashtray.

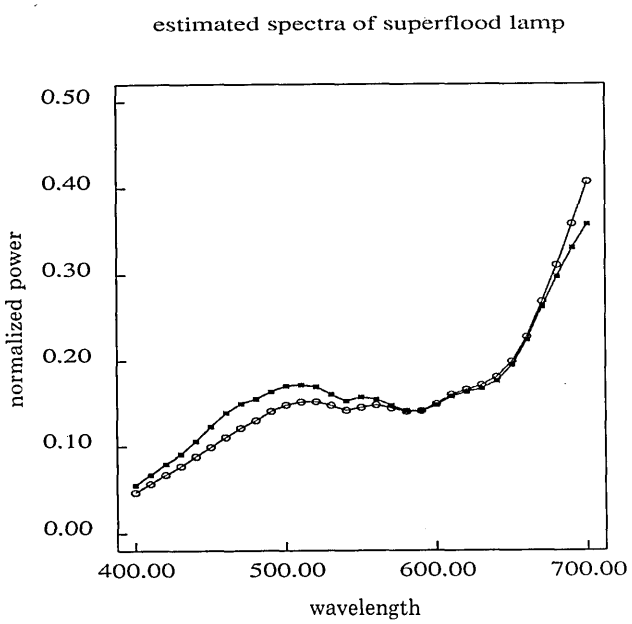

Fig. 12. Estimation results of the illuminant spectral power distribution of a flood lamp. Filled squares represent the estimate from the two plastic objects, and open circles represent the measurement by the standard white.

way as described above, we obtained two basis vectors to determine the plane P(2), where $I(1) = 0.9288$ and $I(2) = 0.9999$. Figure 11 shows plots of these basis vectors.

From these two sets of curves, we have computed the intersection of P(1) and P(2). The SVD of the joint matrix $[\mathbf{u}_1(1), \mathbf{u}_2(1), \mathbf{u}_1(2), \mathbf{u}_2(2)]$ gave the singular values $\lambda_1 = 1.414$, $\lambda_2 = 1.2404$, $\lambda_3 = 0.6792$, and $\lambda_4 = 0.0162$. We conclude that the rank of the joint matrix is 3 and that the planes P(1) and P(2) intersect. The fourth right-hand singular vector $\mathbf{b}_4$ specifies the coordinates of the line. The line vector with a unit length is described as follows:

$$\hat{\mathbf{e}} = 0.4207\mathbf{u}_1(1) + 0.2702\mathbf{u}_2(1) + 0.4567\mathbf{u}_2(2) - 0.2036\mathbf{u}_2(2). \quad (18)$$

Equation (18) expresses an estimate of the spectral power

distribution of the super flood lamp used. The estimate is shown in a solid line marked with black squares in Fig. 12. We compare the estimate with a direct measurement of the spectral power distribution of the light source measured by using a standard white reflectance surface. For the standard white we used a pressed powder of magnesium oxide (MgO). The pressed powder was placed at the same location as the object. The spectral distribution predicted from this measurement is shown by open circles in the figure. A fairly good coincidence between the two curves is seen in the range of middle to long wavelengths.

2. Fruits

We were able to use the same analysis method for the fruits, although the surfaces of the fruits are complicated. The SVD of the 31 × 10 matrix **Y** for the apple gives $\sigma_1 = 3.0513$, $\sigma_2 = 0.8244$, $\sigma_3 = 0.0821, \ldots,$ and $I(2) = 0.9990$. Figure 13 shows the basis curves $\mathbf{u}_1$ and $\mathbf{u}_2$. In contrast, the values for the lemon are $\sigma_1 = 3.1592$, $\sigma_2 = 0.1342$, $\sigma_3 = 0.0272, \ldots,$ and $I(2) = 0.9999$. Figure 14 shows the basis curves. In this case

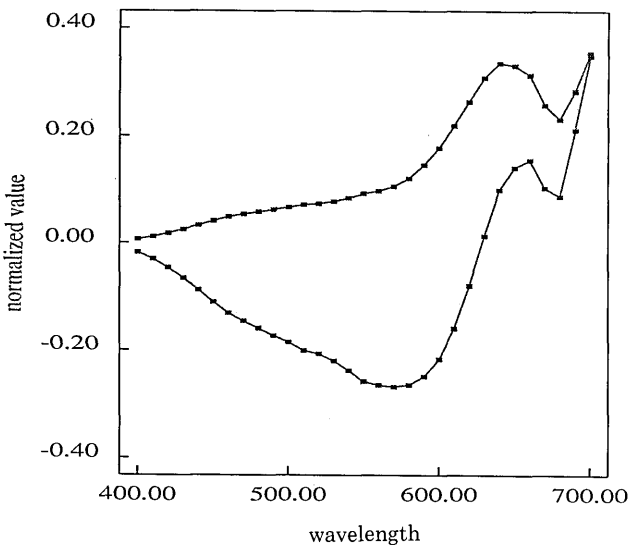

Fig. 13. Basis curves of the measured spectra of the apple.

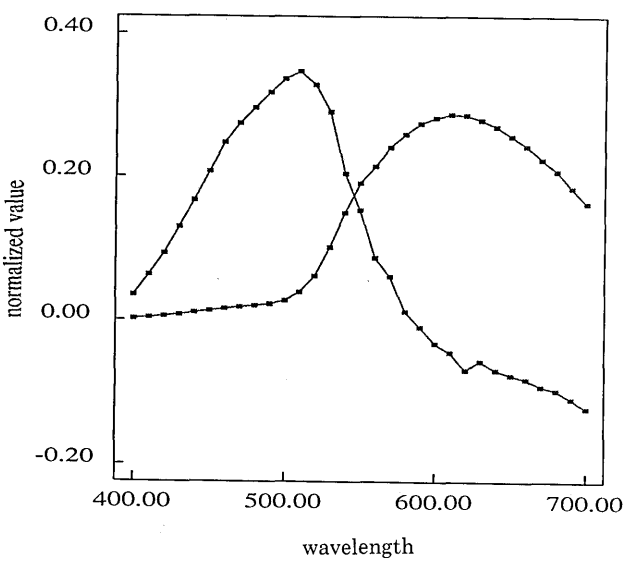

Fig. 14. Basis curves of the measured spectra of the lemon.

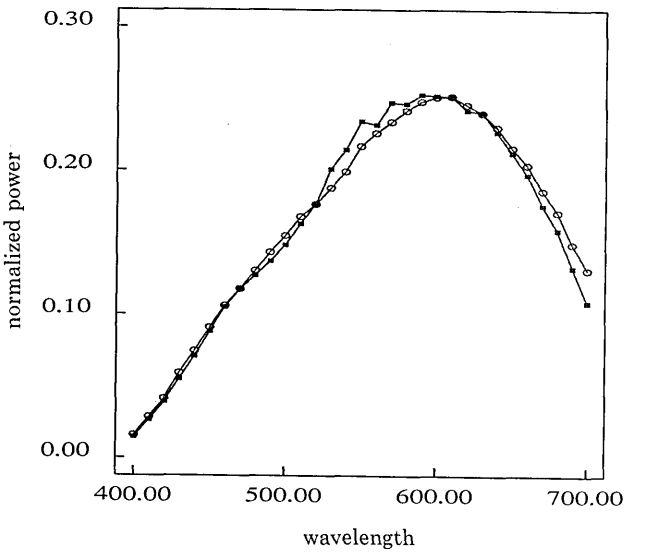

Fig. 15. Estimation results of the illuminant spectral power distribution of a slide projector. Filled squares represent the estimate from the two fruits, and open circles represent the measurement by the standard white.

the joint matrix gives the four values $\lambda_1 = 1.414$, $\lambda_2 = 1.288$, $\lambda_3 = 0.5838$, and $\lambda_4 = 0.0415$. We estimate the spectral power distribution of the slide projector lamp (Fig. 15, filled squares) to be

$$\hat{\mathbf{e}} = 0.4226\mathbf{u}_1(1) + 0.2672\mathbf{u}_2(1) + 0.4655\mathbf{u}_2(2) - 0.1825\mathbf{u}_2(2). \quad (19)$$

The spectral power distribution measured by the reference white is shown by open circles in Fig. 15. A comparison of the two curves shows the reliability of the illuminant spectral estimation for a slide-projector lamp.

These two example measurements are typical of the results that we have obtained with natural products and plastics in our laboratory.

6. DISCUSSION AND CONCLUSION

From our experiments we conclude that the two-component reflection model is adequate for describing color signals from some inhomogeneous materials. For the surfaces that we report here and others that we have measured, the two assumptions of the standard model appear valid. The measured spectral power distributions are described well as falling within a two-dimensional subspace, and the data in the specular highlights are consistent with an interface component that does not affect the spectral composition of the incident light.

We have presented a computational method for estimating the illuminant spectral power distribution based on the two-component reflectance model. An interesting aspect of the computational procedure that we use to measure the illuminant spectrum is that no calibrated reflectance standards are required to measure the light source. Equipped with only the knowledge that the two surfaces are inhomogeneous and with no knowledge of their reflectance functions, the algorithm accurately infers the illuminant spectrum. Since the cost of computational power is often less than that of calibrated, special-purpose materials, this estimation algorithm may prove to be of practical value.

Finally, the algorithm does not require us to establish measurement conditions in which we observe pure specular highlights. Establishing these viewing conditions can be quite difficult. Yet the algorithm estimates the illuminant fairly well under much less elaborate viewing conditions. For example, the fruits are far from being ideal inhomogeneous materials and do not have strong specular reflectance at the spatial resolution of our measurement device. Although the shape of the illuminant spectrum could not be measured directly, since the gloss could never be measured in isolation, an estimate accurate to within a few percent can be extracted from the combined data of the two objects.

ACKNOWLEDGMENTS

This study was performed while S. Tominaga was on leave at Stanford University. The research was supported by NASA grant NCC 2-332 to Stanford University. We thank D. Brainard, H. Lee, and A. Poirson for their helpful comments.

REFERENCES AND NOTES

1. G. J. Klinker, S. A. Shafer, and T. Kanade, "The measurement of highlights in color images," Int. J. Comput. Vision **2,** 7–32 (1988).
2. H.-C. Lee, "Method for computing the scene-illuminant chromaticity from specular highlights," J. Opt. Soc. Am. A **3,** 1694–1699 (1986).
3. M. D'Zmura and P. Lennie, "Mechanisms of color constancy," J. Opt. Soc. Am. A **3,** 1662–1672 (1986).
4. G. Buchsbaum, "A spatial processor model for object color perception," J. Franklin Inst. **310,** 1–26 (1980).
5. M. H. Brill and G. West, "Contributions to the theory of invariance of color under the condition of varying illumination," J. Math. Biol. **11,** 337–350 (1981).
6. L. T. Maloney and B. Wandell, "Color constancy: a method for recovering surface spectral reflectance," J. Opt. Soc. Am. A **3,** 29–33 (1986).
7. R. L. Cook and K. E. Torrance, "A reflectance model for computer graphics," Comput. Graph. **15,** 307–316 (1981).
8. M. Born and E. Wolf, *Principles of Optics* (Pergamon, Oxford, 1983).
9. S. A. Shafer, "Using color to separate reflection components," Color Res. Appl. **10,** 210–218 (1985).
10. H. Lee, E. J. Breneman, and C. P. Schulte, "An experimental study of a color reflection model," Tech. Rep. 229507A (Kodak Research Laboratories, Rochester, N.Y., 1986).
11. All that is required, in fact, is that the specular reflectance function be common and known among the different surfaces. However, it is convenient, and not too inaccurate, to adopt the assumption that the function is constant with respect to wavelength.
12. G. H. Golub and C. F. van Loan, *Matrix Computations* (Johns Hopkins U. Press, Baltimore, Md., 1983).